Published in final edited form as:
Biochim Biophys Acta. 2013 March ; 1827(3): 285–293. doi:10.1016/j.bbabio.2012.11.003.

LYRM7/MZM1L is a UQCRFS1 chaperone involved in the last steps of mitochondrial Complex III assembly in human cells

Ester Sánchez[a,1], **Teresa Lobo**[a,1], **Jennifer L. Fox**[b,2], **Massimo Zeviani**[c], **Dennis R. Winge**[b], and **Erika Fernández-Vizarra**[a,*]

[a]IIS Aragón, Unidad de Investigación Traslacional, Hospital Universitario Miguel Servet, 50009 Zaragoza, Spain

[b]University of Utah Health Sciences Center, Departments of Medicine and Biochemistry, Salt Lake City, Utah 84132, USA

[c]Unit of Molecular Neurogenetics, Fondazione Istituto Neurologico “Carlo Besta” - IRCCS, via Temolo 4, 20126 Milano, Italy

Abstract

The mammalian Complex III (CIII) assembly process is yet to be completely understood. There is still a lack in understanding of how the structural subunits are put together and which additional factors are involved. Here we describe the identification and characterization of LYRM7, a human protein displaying high sequence homology to the *Saccharomyces cerevisiae* protein Mzm1, which was recently shown as an assembly factor for Rieske Fe-S protein incorporation into the yeast cytochrome bc_1 complex. We conclude that human LYRM7, which we propose to be renamed MZM1L (MZM1-like), works as a human Rieske Fe-S protein (UQCRFS1) chaperone, binding to this subunit within the mitochondrial matrix and stabilizing it prior to its translocation and insertion into the late CIII dimeric intermediate within the mitochondrial inner membrane. Thus, LYRM7/MZM1L is a novel human CIII assembly factor involved in the UQCRFS1 insertion step, which enables formation of the mature and functional CIII enzyme.

Keywords

Mitochondrial respiratory chain; Complex III; assembly factor

1. Introduction

Complex III (CIII) or Ubiquinol:cytochrome c oxidoreductase (E.C. 1.10.2.2; the cytochrome bc_1 complex) is the central enzyme of the mitochondrial respiratory chain. It receives electrons from Coenzyme Q, which is reduced mainly by Complex I through NADH-linked substrates and by Complex II through $FADH_2$-linked substrates. CIII then reduces cytochrome c, which transfers the electrons to Complex IV, where molecular

*Corresponding author: Unidad de Investigación Traslacional IACS. Hospital Universitario Miguel Servet. Paseo Isabel la Católica 1-3. 50009 Zaragoza, Spain. Phone: +34 976769565; Fax: +34 976769566; emfernandezvizarra.iacs@aragon.es.
[1]Shared first authorship
[2]Current address: Department of Chemistry and Biochemistry, College of Charleston, Charleston, South Carolina 29424, USA

oxygen is reduced to water. The oxidation and reduction reactions of CIII are coupled to proton translocation from the mitochondrial matrix to the intermembrane space by the so-called Q cycle [1], contributing to the membrane potential necessary for ATP synthesis.

Mammalian CIII possesses a symmetrical dimeric structure in which each "monomer" is composed of 11 different subunits [2, 3], three of which are the catalytic subunits: MT-CYB (Cytochrome b, the only mtDNA-encoded subunit), CYC1 (Cytochrome c_1) and UQCRFS1 (Rieske Fe-S protein).

The CIII assembly process has mainly been studied by using the yeast *S. cerevisiae* as a model, taking advantage of this facultative anaerobic organism and its ability to survive on fermentative substrates when its CIII is non-functional. By analyzing the composition of the sub-complexes present in different yeast deletion strains, a model involving a multi-step process and the formation of different assembly intermediates has been described (reviewed in [4]). In addition, several yeast proteins are known to assist the process by acting in different parts of the assembly pathway [4]. By means of putting all subunits together except the Rieske Fe-S protein (Rip1) and the smallest subunit Qcr10, a considerably stable non-functional "late core" subcomplex, or pre-$CIII_2$ intermediate, is formed. The assembly of the complex is completed when Rip1 is inserted in the last step, followed by Qcr10 [5].

As for all nuclear-encoded mitochondrial proteins, yeast Rip1 is synthesized in the cytoplasm and then imported inside mitochondria. Rip1 is transported completely into the matrix to receive the 2Fe-2S cluster cofactor necessary for its function, and the protein is proteolytically processed in two steps [6]. Differing from yeast, UQCRFS1 in mammals is processed in a single step, and what was originally the pre-sequence is retained as a structural subunit [7]. Translocation of the Rieske Fe-S protein from the matrix to the mitochondrial inner membrane for its insertion into CIII is mediated by the AAA-ATPase Bcs1 [8]. The human ortholog, BCS1L, seems to perform the same function as in yeast, as demonstrated by analysis of CIII assembly in patients carrying deleterious mutations in the *BCS1L* gene [9–11], in which the pre-$CIII_2$ late intermediate lacking UQCRFS1 is accumulated.

Recently, a yeast protein involved in this last Rip1 insertion step has been described [12, 13]. Lack of this protein, Mzm1, is associated with a defect in CIII maturation and reduced CIII activity, as well as very low Rip1 steady-state levels. Furthermore, Mzm1 was demonstrated to interact with Rip1 within the mitochondrial matrix to stabilize it, preventing its proteolytic degradation or its aggregation under conditions in which Rip1 could not be incorporated into CIII [13, 14].

Here, we report the finding and functional characterization of LYRM7, a human protein showing high amino acid sequence homology to the yeast Mzm1. Our results point out that LYRM7 is the MZM1-like (MZM1L) protein, i.e., acting as a Rieske Fe-S protein chaperone in human cells that binds to the subunit within the matrix in a step prior to its insertion into the late pre-$CIII_2$ intermediate. Thus, LYRM7/MZM1L appears to be an assembly factor for the late stage of CIII assembly in humans.

2. Materials and methods

2.1. Cell lines and cell culture

Human primary and immortalized skin fibroblasts, HEK 293T and HeLa cells were grown at 37°C in a 5% CO_2 atmosphere in high-glucose plus glutamine and sodium pyruvate DMEM medium (Gibco-Life Technologies) supplemented with 10% fetal bovine serum (FBS from PAN-Biotech), 1× penicillin-streptomycin (Gibco-Life Technologies) and 50 μg/ml Uridine

(in the case of CIII-deficient cell lines). For the puromycin-resistant cells, a final concentration of 1 μg/ml in the medium was used. Mouse L929 fibroblasts were cultured in the same conditions except for the final FBS concentration, which was 5%.

Primary human skin fibroblasts were immortalized by lentiviral transduction using the pLox-Ttag-ires-TK vector (Tronolab) [15].

2.2. Yeast growth assay

S. cerevisiae expression vectors were constructed to bear the coding sequences for: 1) the human gene *LYRM7* (transcript 1; see section 2.3), followed by 6 histidine repeats and a single Myc tag, 2) the yeast gene *MZM1*, followed by a single Myc tag and 6 histidine repeats, and 3) the yeast gene *SDH6*, followed by 6 histidine repeats and a single Myc tag. These coding sequences were cloned into a common high-copy-number pRS426 plasmid bearing a *URA3* selection marker and expressed under the control of the yeast *MET25* promoter and *CYC1* terminator sequences [16]. These plasmids as well as an empty vector control were transformed into wild-type and Δ*mzm1* deletion yeast strains of the BY4741 genetic background via a variation of the lithium acetate procedure [17]. Transformed cells were grown on selective plates containing Brent supplement mixture lacking uracil (Sunrise Science Products, San Diego, CA) plus 2% glucose, and colonies were inoculated into 4-ml cultures of the same media, grown overnight, and spotted onto selective plates containing either 2% glucose or 2% glycerol/2% lactate at equivalent optical densities (at 600 nm) in a 10-fold serial dilution. Plates were incubated at 30°C or 37°C and photographed after ~48 h (glucose) and ~144 h (glycerol-lactate) of growth.

2.3. LYRM7 constructs

cDNA was obtained by using the GoScript reverse transcription system (Promega), using total RNA extracted from cultured cells with TRIzol reagent (Invitrogen). PCR products were produced using cDNA as the template with specific primers: hLYRM7-MluI-Fw: 5'-CTTTACGCGTCAGTCTTTGATTGGTTGCTG-3' and hLYRM7-SalI-Rv: 5'-CCCCGTCGACCTTGTTGTATTCTAGAAAAC-3'; mLyrm7-MluI-Fw: 5'-CTTTACGCGTGGGGAGCCATGGGTCAG-3' and mLyrm7-SalI-Rv: 5'-CCCTGTCGACAGAGATGGGTTTATCCTGG-3'. The obtained PCR products were cloned into the pCR2.1 TA cloning system (Invitrogen). Sequence checked clones containing the two insert variants (LYRM7-001 and LYRM7-003) were used as templates for the amplification to add the HA tag at the C-terminus of the putative protein products, using the same hLYRM7-MluI-Fw primer and hLYRM7-001-HA-SalI-Rv: 5'-CCCGTCGACTCAAGCGTAATCTGGAACATCGTATGGGTATTGCTTCTGAGTTGGTGCATC-3' or hLYRM7-003-HA-SalI-Rv: 5'-CCCGTCGACTCAAGCGTAATCTGGAACATCGTATGGGTACAAGAAGGTCTTTCCTAGGG-3'. The PCR products were cloned into the pCR2.1 TA cloning system (Invitrogen). Inserts with the correct sequences were subsequently cloned into a lentiviral expression vector derived from pWPXLd (Tronolab), in which the GFP sequence was substituted by a puromycin resistance cassette (pWPXLd-ires-Puro^R).

2.4. Lentiviral transduction

Lentiviral particles containing the LYRM7-001-HA/pWPXLd-ires-Puro^R, LYRM7-003-HA/pWPXLd-ires-Puro^R or the empty pWPXLd-ires-Puro^R vectors were generated in HEK 293T packaging cells, and HeLa cells were transduced with the former as described [18]. Twenty-four hours after transduction, cells were selected for puromycin resistance (section 2.1).

2.5. Isolation and subfractionation of mitochondria

Mitochondrial preparations from transduced HeLa cells were obtained as described [19]. For subfractionation of mitochondria, to separate the soluble and membranous fractions, freshly isolated mitochondria were sonicated three times and then centrifuged at 100,000×g for 30 minutes at 4°C to separate the supernatant containing the soluble proteins and the membrane pellet [20]. To split the peripherally bound from the integral membrane proteins in the pellet from the previous step, the samples were resuspended in a buffer containing 0.1 M Na_2CO_3, pH 10.5, 0.25 M sucrose and 0.2 mM EDTA; incubated for 30 min on ice and then centrifuged at 100,000×g for 30 minutes at 4°C, to separate the pellet from the supernatant [21].

2.6. Immunoprecipitation

Approximately 500 μg of mitochondrial protein isolated from HeLa cells either transduced with the empty pWPXLd-ires-Puro^R vector or overexpressing LYRM7-001-HA (MZM1L-HA), were lysed in PBS with 140 mM NaCl, 1% n-Dodecyl β-D-maltoside (DDM) and protease inhibitor cocktail (Sigma), during 30 minutes on ice. The lysate was cleared by centrifugation at 20,000×g for 30 minutes and divided into three aliquots, which were each incubated with 1.5 μg of high affinity anti-HA antibody (Roche), anti-Rieske protein antibody (Molecular Probes-Invitrogen) or mouse serum IgGs (Sigma) for 5 hours at 4°C. Immunoprecipitation was achieved by adding pre-washed Protein G-Sepharose 4B beads (Invitrogen) and incubating an additional 2 hours at 4°C. The co-immunoprecipitates were washed three times in astringent conditions (PBS with 400 mM NaCl, 0.1% DDM and protease inhibitor cocktail) and once in low salt conditions (PBS with 140 mM NaCl, 0.1% DDM and protease inhibitor cocktail). Proteins were finally eluted from the beads with 2× Laemmli Sample Buffer and heated at 95°C for 5 minutes.

2.7. Protein electrophoresis, Western Blot and immunodetection

Total protein extracts from cultured cells or fractions were resolved under denaturing conditions using 16.5% polyacrylamide Tricine-SDS-PAGE [22] or standard 15% polyacrylamide SDS-PAGE.

Blue-Native Gel Electrophoresis (BNGE) was performed using mitoplast samples prepared by lysing cells in the presence of digitonin, followed by a final solubilization with 1% DDM as described [23]. The complexes were resolved in 5–13% gradient polyacrylamide native gels [24]. For the second denaturing dimension, 16.5% polyacrylamide Tricine-SDS-PAGE preceded by a 10% polyacrylamide stacking gel was used [9].

The gels were electroblotted to PVDF membranes, and the immobilized proteins were immunodetected using specific antibodies as indicated in each case. Anti-Core 1 (CIII subunit 1), anti-Core 2 (CIII subunit 2), anti-COI (Complex IV subunit I) and Mitoprofile (Total OXPHOS Blue Native WB Antibody Cocktail) were from Mitosciences, anti-Rieske protein was from Molecular Probes-Invitrogen, anti-BCS1L was from Proteintech Group, High Affinity anti-HA was from Roche and anti-Actin and anti-LYRM7 were from Sigma.

2.8. Respiratory chain enzymatic activity measurements

For the biochemical kinetic reaction assays, digitonin-solubilized cell samples were used [25]. Individual CIII (decylubiquinol:cytochrome c reductase), CIV (cytochrome c oxidase) and citrate synthase (CS) activities were measured as described [26], with slight modifications. The reactions were performed in 96-well plates in a final volume of 200 μl and measured in a Synergy HT Multi-Mode Microplate Reader (BioTek Instruments).

2.9. Statistical analyses

First, analysis of variance (ANOVA) was used to test the difference between the mean values of the CIII and CIV activity measurements in the different cell lines, normalized by citrate synthase. Secondly, the groups were compared pair-wise using the Post-Hoc LSD test. P values < 0.05 were considered significant. The statistical analyses were performed using the SPSS 16.0 software for Windows.

2.10. Internet resources

National Center for Biotechnology Information: http://www.ncbi.nlm.nih.gov/guide/

Ensembl Genome Browser: http://www.ensembl.org/index.html

Protein Knowledgebase (UniProtKB): http://www.uniprot.org/

ClustalW2 Multiple Sequence Alignment: http://www.ebi.ac.uk/Tools/msa/clustalw2/

Human MitoCarta: http://www.broadinstitute.org/pubs/MitoCarta/human.mitocarta.html

Mouse MitoCarta: http://www.broadinstitute.org/pubs/MitoCarta/mouse.mitocarta.html

ExPASy compute pI/Mw tool: http://web.expasy.org/compute_pi/

3. Results

3.1. Identification of the Mzm1 human and mouse orthologs

Performing a protein BLAST analysis using the Mzm1p amino acid sequence (NCBI Protein Reference Sequence ID: NP_010781) resulted in the identification of the LYR motif containing 7 or human LYRM7 (NCBI Protein ID: NP_859056) and mouse Lyrm7 (NCBI Protein ID: NP_083603) proteins as sequence homologs (Figure 1A). The coding sequence for both species' proteins was amplified from cDNA using specific primers upstream of the initiation codon and downstream of the stop codon (see section 2.3). After screening 20 bacterial colonies transformed with each of the cloned PCR products, two different inserts were detected in those amplified from human cDNA from either primary skin fibroblasts or HEK 293T cells. Of the three predicted transcripts for the human chromosome 5 gene listed in the Ensembl data base (Ensembl Gene ID: ENSG00000186687), which should be amplified with the primers used, we were able to obtain those corresponding to transcript 1 (LYRM7-001; Ensembl Transcript ID: ENST00000379380) and transcript 3 (LYRM7-003; Ensembl Transcript ID: ENST00000507584). Transcript 1 encodes a 104 amino acid polypeptide, which is the protein expected to be the Mzm1 human ortholog, while transcript 3 is a splicing variant where exon 4 is missing and is predicted to produce a 63 amino acid protein. In the case of the mouse samples from cultured L929 cells, we were able to amplify only one cDNA, corresponding to the Lyrm7-005 transcript (Ensembl Transcript ID: ENSMUST00000144164) of the mouse chromosome 11 gene (Ensemble Gene ID: ENSMUSG00000020268) encoding the 104 amino acid Mzm1 mouse homolog.

3.2. Respiratory growth in Δmzm1 yeast strain is restored by LYRM7

Yeast strains lacking Mzm1 (Δ*mzm1*) show defective growth on non-fermentable carbon sources due to a defect in respiration linked to a CIII deficiency, which is much more marked at 37°C [12, 13]. Some human proteins involved in mitochondrial respiratory chain biogenesis, which are yeast factor functional homologs, are capable of complementing respiratory defects in *S. cerevisiae* when the *H. sapiens* allele is introduced in the deletion mutant yeast cells. This is the case, for example, for the CIII assembly factor BCS1L [9, 27].

To test for any such complementation in the case of LYRM7, the human allele encoding the 104 amino acid LYRM7-001 was introduced in the Δ*mzm1* cells. As can be seen in Figure

1B, human LYRM7 restored the ability of the mutant yeast strain to grow on non-fermentable media at 37°C, as did transformation with the yeast *MZM1*. Another yeast protein included in the LYR motif family, *SDH6* (human ortholog SDHAF1), failed to restore the growth in Δ*mzm1* cells. Therefore, the capacity of human LYRM7 to complement for the yeast respiration-dependent growth defect induced by the lack of Mzm1 suggested that the human protein not only shows a high sequence homology but that it could also function in a similar manner as yeast Mzm1.

3.3. Overexpression of LYRM7/MZM1L in human cells produces a change in the UQCRFS1 submitochondrial distribution and impairs CIII maturation

The HA tagged versions of LYRM7-001 and LYRM7-003 were overexpressed in HeLa cells by lentiviral transduction. Western Blot analyses of total protein extracts from cells transduced with the empty vector and with both LYRM7 constructs showed that only in the case of transcript 1, a protein product was detected using an anti-HA antibody (Figure 2A), even though LYRM7-003-HA was stably expressed at the mRNA level (Figure 2B).

Cells overexpressing LYRM7-001-HA, which will be referred to as MZM1L-HA from now on, contain similar steady-state levels of UQCRFS1 (Rieske Fe-S protein) and other CIII subunits compared to the cells transduced with the empty vector or with the LYRM7-003-HA construct (Figure 2A).

LYRM7 is included in the mitochondrial proteome compendium MitoCarta [28]. By cell subfractionation we aimed to confirm this subcellular localization and determine in which mitochondrial fraction, soluble or membranous, it was found. In SDS-polyacrylamide gels, LYRM7 was detected in mitochondrial fractions when visualized by either anti-LYRM7 or anti-HA immunoreactivity. In the cells overexpressing LYRM7/MZM1L-HA, two bands appeared when using the specific anti-LYRM7 antibody, the one corresponding to the endogenous protein at the expected size of around 12 kDa (theoretical mass: 11,955 Da) and the other one migrating a little slower consistent with the HA tagged protein theoretical mass of 13,039 Da (Figure 2A and C). In addition, another band appeared to react with the anti-HA antibody located close to the 37 kDa molecular mass band (Figures 2C, 5 and 6). The endogenous LYRM7/MZM1L and the tagged MZM1L-HA showed the same subcellular and submitochondrial distribution in the different tested fractions (Figure 2C). Thus, both were detected mainly in the soluble mitochondrial fraction (lanes 4 and 11) where the mitochondrial matrix marker SOD2 was present, concordant with the matrix submitochondrial localization of Mzm1 in yeast [12]. However, a fraction of LYRM7/MZM1L was associated with the mitochondrial membranes (Figure 2C, lanes 5 and 12) although mostly peripherally, because considerable amounts were extracted from the membrane pellet by sodium carbonate treatment (Figure 2C, lanes 6 and 13).

HeLa cells overexpressing MZM1L-HA were found to contain elevated levels of UQCRFS1 in the mitochondrial soluble fraction (lane 11) than in the membrane pellet (lane 12) relative to cells transduced with the empty vector, where only a small proportion of the detected UQCRFS1 was in the soluble fraction (lane 4) and most of it was in the insoluble membrane pellet (lane 5 in Figure 2C).

The presence of MZM1L-HA in a macromolecular complex was tested by BNGE. The overexpressed tagged protein was present in a low molecular weight complex of less than 100 kDa, migrating to the lowest part of the native polyacrylamide gradient gel (Figures 3A and 5A).

High levels of MZM1L-HA overexpression led to a decrease in the amount of UQCRFS1 associated with $CIII_2$. The signal corresponding to UQCRFS1 was lower in MZM1L-HA

cells compared to cells containing the empty vector with a marked diminution in the abundance of the UQCRFS1-containing $CIII_2$+CIV supercomplex. In fact, the amount of UQCRFS1 detected in the $CIII_2$ and $CIII_2$+CIV bands was inversely proportional to the MZM1L-HA level, as seen in the cells infected with decreasing amounts of viral particles (Figure 3A). On the other hand, the amount of detected UQCRC2 (Core2 subunit) was comparable in all the samples. In the samples where Rieske Fe-S protein insertion was reduced, there was an accumulation of the late core pre-$CIII_2$, either alone or in association with CIV. These species lacking UQCRFS1 appeared to co-migrate in the Blue-Native gels with the corresponding fully assembled complexes containing UQCRFS1. This co-migration is indicated in Figure 3A, where anti-Core2 detects both the UQCRFS1-less $CIII_2$ and the holo-$CIII_2$ with or without CIV (pre-$CIII_2$+$CIII_2$+CIV and pre-$CIII_2$+$CIII_2$, respectively). This situation resembled what is observed when the reduced incorporation of UQCRFS1 occurs due to mutations in *BCS1L* [9]. In addition, stronger signals corresponding to UQCRC1 and UQCRC2-containing subcomplexes, appeared in the highly expressing MZM1L-HA transduced lines (Figure 3B), indicating either a decreased stability or an impaired CIII assembly in these samples. Furthermore, in the cells expressing high amounts of MZM1L-HA (100%, 50% and 25% of the virus titration) an anomalous band migrating between $CIII_2$+CIV and $CIII_2$ appeared in the immunodetection with the anti-Core 2 antibody (Figure 3A). This intermediate band (sub-$CIII_2$+CIV) seemed to represent the association of a partially assembled CIII with CIV, as it contains UQCRC1, UQCRC2 and MT-CO1 (Figure 3B) and its emergence could be associated with defective UQCRFS1 incorporation, as it was also evident in BCS1L-mutated patient fibroblasts [9].

Because UQCRFS1 is the last catalytic subunit to be incorporated into CIII in the assembly pathway, if it is not properly inserted, the complex cannot be functional. In accord with observations from the BNGE, western blot and immunodetection analyses, CIII activity was reduced in the cell lines where the MZM1L-HA expression was higher (Figure 4A). On the other hand, the pair-wise comparison of the measurements in the cells infected with 6.5% of the total virus titration, showed a statistically significant elevation in CIII activity with respect to the other cell lines generated using increasing virus concentrations (indicated in Figure 4A). CIII enzymatic activity was also higher in the cell line obtained after transduction with 12.5% of the total virus titration. Therefore, lower expression levels of the exogenous tagged polypeptide may contribute to the endogenous protein function, helping in the stabilization/incorporation of UQCRFS1 into the pre-$CIII_2$ intermediate.

3.4. MZM1L and UQCRFS1 physically interact

Denaturing 2D analyses after a first BNGE dimension clearly showed the accumulation of the UQCRFS1 signal in positions corresponding to low molecular weight complexes (Figure 5A), which was more intense in the samples in which MZM1L-HA was overexpressed (Figures 3B and 5A). The signals corresponding to the anti-HA antibody were also visualized in these low molecular weight positions in the first dimension, which seemed to indicate a MZM1L-HA co-migration with the UQCRFS1-containing intermediate, as a Rip1+Mzm1 complex is also observed by 2D analysis in yeast [14].

In order to test whether the UQCRFS1 and MZM1L-HA signal coincidence in the low molecular weight protein complex by BNGE was only due to co-migration in the gels or if it meant a physical interaction between both proteins, we performed co-immunoprecipitation assays. Immunoprecipitation from mitochondrial lysates, isolated from HeLa cells overexpressing MZM1L-HA and using an anti-HA antibody, also pulled down UQCRFS1, as it was specifically detected in the co-immunoprecipitate. Conversely, when the immunoprecipitation assay was performed using an anti-Rieske protein antibody, the HA signal corresponding to the tagged MZM1L protein was detected in the pulled-down

fraction, while it was absent in the control reaction using generic mouse IgGs (Figure 5B). These data strongly support the existence of a UQCRFS1+MZM1L-HA protein complex.

3.5. MZM1L stabilizes UQCRFS1 in a step prior to the BCS1L-mediated insertion into CIII

Most of the mitochondrial CIII deficiency (OMIM 124000) cases described to date are due to mutations in the *BCS1L* gene (OMIM 603647). BCS1L is a required factor for the correct biogenesis of CIII [29], as its defects are correlated with low UQCRFS1 incorporation into the pre-$CIII_2$ late intermediate [9, 11]. MZM1L-HA was overexpressed in immortalized skin fibroblasts derived from Patients 1 and 2, which carry pathogenic BCS1L mutations [9]. These cells showed low UQCRFS1 amounts together with the presence of UQCRC1 (Core 1)- and UQCRC2 (Core 2)-containing subcomplexes, which were absent in the control samples [9]. MZM1L-HA overexpression in these patient cells produced an increase in UQCRFS1 steady-state levels (Figure 6A). However, this increase was correlated with the accumulation of the UQCRFS1 at the low molecular weight intermediate/s rather than with a higher incorporation of the catalytic subunit into $CIII_2$ or an amelioration of the UQCRC1 assembly state (Figure 6B). These observations suggested that MZM1L bound to and was able to stabilize UQCRFS1 in the case of its failed translocation to the inner membrane due to BCS1L malfunction. This behavior of MZM1L is consistent with a similar observation in yeast lacking the gene for *BCS1* [14].

4. Discussion

Mitochondrial Complex III assembly in mammalian cells is not a well-known process, as there is still a lack of information about how the subunits are put together to give rise to the functional mature enzyme and what factors are involved in the assembly. In fact, up to now the only two mammalian proteins known to play a role in CIII biogenesis are BCS1L and TTC19, which were discovered by analyzing human pathological cases associated with CIII deficiency [27, 30]. The yeast *Saccharomyces cerevisiae* is extremely useful as a model organism to study mitochondrial respiratory chain biogenesis thanks to the feasibility of its genetic manipulation and its ability to grow on fermentable carbon sources when the OXPHOS system is defective. Much of the knowledge about the Complex IV assembly factors has been obtained by identifying such proteins in yeast and then looking for the mammalian homologs [31]. However, there are significant differences between yeast and mammals, especially in the peri-translational processes of the mitochondrially encoded subunits where the proteins that exert these functions are not exact orthologs, and new factors not related to the yeast proteins are being discovered in human cells [32, 33].

Complex III, or the cytochrome bc_1 complex, is structurally very similar between yeast and mammals, although the mammalian enzyme contains an extra subunit, which is the cleaved UQCRFS1 (Rieske Fe-S protein) pre-sequence that is retained as a structural part of the complex [7]. A quite detailed assembly model has been described in yeast by studying the subcomplexes formed in different deletion strains for each of the structural subunits [34]. In addition, several factors assisting the assembly process at different points have been identified [4]. The best characterized factor is Bcs1, which translocates the catalytic protein Rip1 (Rieske Fe-S protein) from the matrix to the mitochondrial inner membrane in order to be inserted into a late core intermediate [8], which is nearly the fully assembled complex, only lacking Rip1 and the smallest accessory subunit Qcr10 (which is inserted after the catalytic protein) [5]. The human counterpart of this essential assembly factor, BCS1L, seems to perform the same function [9]. Another human protein, TTC19, which does not appear to have a yeast homolog, is necessary for the correct biogenesis of CIII, but its exact role in the process is yet to be elucidated [30].

In this report we describe the identification and characterization of a new protein that we show to be involved in CIII assembly in human cells, which is the Mzm1 homolog. Yeast Mzm1 has been recently described to function in the late steps of bc_1 complex assembly [12]. Functional studies in yeast describe how Mzm1 is a LYR motif-containing chaperone that stabilizes Rip1 prior to its inner membrane insertion mediated by Bcs1, a function which is especially necessary at elevated temperatures [13, 14].

LYR motif –containing 7 (LYRM7) is a protein of the "Complex I LYR family," whose main characteristic is the N-terminal LYR motif important for protein function and which includes members such as NDUFA6, NDUFB9 (Complex I structural subunits) and the CII assembly factor SDHAF1 [35], all of which are related to Fe-S cluster proteins. Our results indicate that LYRM7 transcript variant 1, encoding a 104-amino acid polypeptide, produces a mitochondrial protein that binds and stabilizes UQCRFS1 in the mitochondrial matrix, for which we consider it the human Mzm1 functional homolog or MZM1-like protein (MZM1L).

Several lines of evidence allow us to make this statement: First, expression of the human protein is able to restore respiratory growth in yeast cells devoid of the endogenous Mzm1. This result indicates that LYRM7/MZM1L possesses a homologous function, as it is able to compensate for the bc_1 complex defect induced by the lack of Mzm1, which is mainly characterized by the loss of Rip1 [12, 13]. Second, overexpression of the protein increases UQCRFS1 steady-state levels in the BCS1L defective fibroblasts. Third, high levels of MZM1L provoke the accumulation of UQCRFS1 in a soluble mitochondrial fraction, in contrast to the situation in which MZM1L levels are lower, where only a small proportion of the subunit is soluble and most of it is tightly bound to the mitochondrial inner membrane (Figure 2C). This observation indicates than in the case of MZM1L overexpression, most of the UQCRFS1, although not all, must be located in the matrix together with the chaperone, making it more difficult for the subunit to reach the inner membrane. Lastly, MZM1L physically interacts with UQCRFS1, as demonstrated by their co-migration in the Blue-Native gels and by their co-immunoprecipitation. UQCRFS1 is mostly present in the MZM1L-HA-containing subcomplex when the latter is overexpressed, and this same subcomplex is also detected with the anti-Rieske protein antibody in the control cells (transduced with the empty vector) in much lower proportions (Figures 3B and 5B).

Furthermore, high MZM1L-HA expression levels even produced a decrease in CIII activity in HeLa cells due to a reduced UQCRFS1 incorporation into CIII, as observed by the lighter signal detected for this subunit in the BNGE, WB and immunodetections (Figure 3A). The signal was reduced in an inverse proportion to the MZM1L-HA expression levels, and the impaired incorporation was more evident in the $CIII_2$+CIV supercomplex band. This finding is compatible with the observation by kinetic studies and BNGE that the incorporation dynamics of UQCRFS1 were slower in the $CIII_2$ + CIV and respirasome bands than in the isolated $CIII_2$ band [36].

All the observations strongly suggest that UQCRFS1 stays retained in the matrix and bound to MZM1L-HA within the low molecular weight intermediate. One could argue that this result could be due to a dominant negative effect because the addition of the HA tag is disturbing the function of MZM1L. However, the addition of a C-terminal tag to the yeast Mzm1 protein did not have any deleterious effect on its function, nor did the addition of a C-terminal tag to the human MZM1L expressed in yeast [13] (Figure 1B). In addition, by modulating the MZM1L-HA overexpression levels (lowering the virus titration while infecting the cells), it was shown that the HeLa cells where MZM1L-HA expression levels were the lowest exhibited statistically significant higher CIII enzymatic activities, in comparison with the control cells and, evidently, in comparison with the lines with high

MZM1L-HA expression. This result suggests that the tagged protein, when expressed in the right amounts, is able to cooperate with the endogenous factor to stabilize UQCRFS1 for its incorporation into a mature CIII. This finding also indicates that the right stoichiometry of the factor is necessary for its correct function, as when there is an excessive amount of MZM1L, considerable quantities of UQCRFS1 are retained in the wrong compartment, which is counterproductive for correct CIII maturation. Accordingly, MZM1L-HA overexpression was able to increase the low UQCRFS1 levels present in BCS1L-mutated cells, but it could not ameliorate CIII assembly, as the amount of UQCRFS1 incorporated into mature $CIII_2$ remained low and the accumulation of UQCRFS1 in the MZM1L-HA-overexpressing patient cells occurred in the low molecular weight intermediate.

In conclusion, the results shown in this report allow us to introduce a new player, MZM1L, in the last step of the mammalian CIII assembly pathway, where pre-CIII is matured to become the functional enzyme (Figure 7). In addition, this study opens the possibility of screening for pathogenic mutations in the LYRM7/MZM1L gene in yet unresolved mitochondrial disease cases associated with CIII deficiency. Additionally, there is still much work needed to be done in order to identify the pathway and additional factors taking part in the biogenesis of this mitochondrial respiratory chain central complex.

Acknowledgments

The authors are grateful to Nieves Movilla, Patricio Fernández-Silva and José A. Enríquez for their support and Ester Perales-Clemente for the construction of the pWPXLd-ires-Puro^R vector. We would also like to thank M. Pilar Bayona-Bafaluy and Carlo Viscomi for critically reading the manuscript. Our research was supported by a “Miguel Servet” Grant (CP09/00156) from the Instituto de Salud Carlos III (Ministerio de Economía y Competitividad), “Marie Curie” European Reintegration Grant (PERG04-GA-2008-239372) and Association Française contre les Myopathies Trampoline Grant (AFM 14921) and Research Grant (AFM 16086) to E.F.-V. This work was also supported by grant GM083292 to D.R.W., and J.L.F. was supported by training grant T32 HL007576-25.

References

1. Crofts AR, Holland JT, Victoria D, Kolling DR, Dikanov SA, Gilbreth R, Lhee S, Kuras R, Kuras MG. The Q-cycle reviewed: How well does a monomeric mechanism of the bc(1) complex account for the function of a dimeric complex? Biochim.Biophys.Acta. 2008; 1777:1001–1019. [PubMed: 18501698]
2. Schagger H, Link TA, Engel WD, von Jagow G. Isolation of the eleven protein subunits of the bc1 complex grom beef heart. Methods Enzymol. 1986; 126:224–237. [PubMed: 2856130]
3. Iwata S, Lee JW, Okada K, Lee JK, Iwata M, Rasmussen B, Link TA, Ramaswamy S, Jap BK. Complete structure of the 11-subunit bovine mitochondrial cytochrome bc1 complex. Science. 1998; 281:64–71. [PubMed: 9651245]
4. Smith PM, Fox JL, Winge DR. Biogenesis of the cytochrome bc(1) complex and role of assembly factors. Biochim Biophys Acta. 2012; 1817:276–286. [PubMed: 22138626]
5. Zara V, Conte L, Trumpower BL. Evidence that the assembly of the yeast cytochrome bc1 complex involves the formation of a large core structure in the inner mitochondrial membrane. Febs J. 2009; 276:1900–1914. [PubMed: 19236481]
6. Hartl FU, Schmidt B, Wachter E, Weiss H, Neupert W. Transport into mitochondria and intramitochondrial sorting of the Fe/S protein of ubiquinolcytochrome c reductase. Cell. 1986; 47:939–951. [PubMed: 3022944]
7. Brandt U, Yu L, Yu CA, Trumpower BL. The mitochondrial targeting presequence of the Rieske iron-sulfur protein is processed in a single step after insertion into the cytochrome bc1 complex in mammals and retained as a subunit in the complex. J.Biol.Chem. 1993; 268:8387–8390. [PubMed: 8386158]

8. Wagener N, Ackermann M, Funes S, Neupert W. A Pathway of Protein Translocation in Mitochondria Mediated by the AAA-ATPase Bcs1. Mol Cell. 2011; 44:191–202. [PubMed: 22017868]
9. Fernandez-Vizarra E, Bugiani M, Goffrini P, Carrara F, Farina L, Procopio E, Donati A, Uziel G, Ferrero I, Zeviani M. Impaired complex III assembly associated with BCS1L gene mutations in isolated mitochondrial encephalopathy. Hum.Mol.Genet. 2007; 16:1241–1252. [PubMed: 17403714]
10. Hinson JT, Fantin VR, Schonberger J, Breivik N, Siem G, McDonough B, Sharma P, Keogh I, Godinho R, Santos F, Esparza A, Nicolau Y, Selvaag E, Cohen BH, Hoppel CL, Tranebjaerg L, Eavey RD, Seidman JG, Seidman CE. Missense mutations in the BCS1L gene as a cause of the Bjornstad syndrome. N.Engl.J.Med. 2007; 356:809–819. [PubMed: 17314340]
11. Moran M, Marin-Buera L, Gil-Borlado MC, Rivera H, Blazquez A, Seneca S, Vazquez-Lopez M, Arenas J, Martin MA, Ugalde C. Cellular pathophysiological consequences of BCS1L mutations in mitochondrial complex III enzyme deficiency. Hum Mutat. 2010; 31:930–941. [PubMed: 20518024]
12. Atkinson A, Khalimonchuk O, Smith P, Sabic H, Eide D, Winge DR. Mzm1 influences a labile pool of mitochondrial zinc important for respiratory function. J Biol Chem. 2010; 285:19450–19459. [PubMed: 20404342]
13. Atkinson A, Smith P, Fox JL, Cui TZ, Khalimonchuk O, Winge DR. The LYR Protein Mzm1 Functions in the Insertion of the Rieske Fe/S Protein in Yeast Mitochondria. Mol Cell Biol. 2011; 31:3988–3996. [PubMed: 21807901]
14. Cui TZ, Smith PM, Fox JL, Khalimonchuk O, Winge DR. Late-Stage Maturation of the Rieske Fe/S Protein: Mzm1 Stabilizes Rip1 but Does Not Facilitate Its Translocation by the AAA ATPase Bcs1. Mol Cell Biol. 2012; 32:4400–4409. [PubMed: 22927643]
15. Salmon P, Oberholzer J, Occhiodoro T, Morel P, Lou J, Trono D. Reversible immortalization of human primary cells by lentivector-mediated transfer of specific genes. Mol Ther. 2000; 2:404–414. [PubMed: 11020357]
16. Mumberg D, Muller R, Funk M. Regulatable promoters of Saccharomyces cerevisiae: comparison of transcriptional activity and their use for heterologous expression. Nucleic Acids Res. 1994; 22:5767–5768. [PubMed: 7838736]
17. Gietz RD, Schiestl RH. High-efficiency yeast transformation using the LiAc/SS carrier DNA/PEG method. Nat Protoc. 2007; 2:31–34. [PubMed: 17401334]
18. Perales-Clemente E, Bayona-Bafaluy MP, Perez-Martos A, Barrientos A, Fernandez-Silva P, Enriquez JA. Restoration of electron transport without proton pumping in mammalian mitochondria. Proc.Natl.Acad.Sci.U.S.A. 2008; 105:18735–18739. [PubMed: 19020091]
19. Fernández-Vizarra E, Ferrín G, Pérez-Martos A, Fernández-Silva P, Zeviani M, Enríquez JA. Isolation of mitochondria for biogenetical studies: An update. Mitochondrion. 2010; 10:253–262. [PubMed: 20034597]
20. Ghezzi D, Viscomi C, Ferlini A, Gualandi F, Mereghetti P, DeGrandis D, Zeviani M. Paroxysmal non-kinesigenic dyskinesia is caused by mutations of the MR-1 mitochondrial targeting sequence. Hum Mol Genet. 2009; 18:1058–1064. [PubMed: 19124534]
21. Satoh M, Hamamoto T, Seo N, Kagawa Y, Endo H. Differential sublocalization of the dynamin-related protein OPA1 isoforms in mitochondria. Biochem Biophys Res Commun. 2003; 300:482–493. [PubMed: 12504110]
22. Schagger H. Tricine-SDS-PAGE. Nat.Protoc. 2006; 1:16–22. [PubMed: 17406207]
23. Nijtmans LG, Henderson NS, Holt IJ. Blue Native electrophoresis to study mitochondrial and other protein complexes. Methods. 2002; 26:327–334. [PubMed: 12054923]
24. Wittig I, Braun HP, Schagger H. Blue native PAGE. Nat.Protoc. 2006; 1:418–428. [PubMed: 17406264]
25. Tiranti V, Munaro M, Sandona D, Lamantea E, Rimoldi M, DiDonato S, Bisson R, Zeviani M. Nuclear DNA origin of cytochrome c oxidase deficiency in Leigh's syndrome: genetic evidence based on patient's-derived rho degrees transformants. Hum Mol Genet. 1995; 4:2017–2023. [PubMed: 8589677]

26. Kirby DM, Thorburn DR, Turnbull DM, Taylor RW. Biochemical assays of respiratory chain complex activity. Methods Cell Biol. 2007; 80:93–119. [PubMed: 17445690]
27. de Lonlay P, Valnot I, Barrientos A, Gorbatyuk M, Tzagoloff A, Taanman JW, Benayoun E, Chretien D, Kadhom N, Lombes A, de Baulny HO, Niaudet P, Munnich A, Rustin P, Rotig A. A mutant mitochondrial respiratory chain assembly protein causes complex III deficiency in patients with tubulopathy, encephalopathy and liver failure. Nat.Genet. 2001; 29:57–60. [PubMed: 11528392]
28. Pagliarini DJ, Calvo SE, Chang B, Sheth SA, Vafai SB, Ong SE, Walford GA, Sugiana C, Boneh A, Chen WK, Hill DE, Vidal M, Evans JG, Thorburn DR, Carr SA, Mootha VK. A mitochondrial protein compendium elucidates complex I disease biology. Cell. 2008; 134:112–123. [PubMed: 18614015]
29. Fernandez-Vizarra E, Tiranti V, Zeviani M. Assembly of the oxidative phosphorylation system in humans: What we have learned by studying its defects. Biochim.Biophys.Acta. 2009; 1793:200–211. [PubMed: 18620006]
30. Ghezzi D, Arzuffi P, Zordan M, Da Re C, Lamperti C, Benna C, D'Adamo P, Diodato D, Costa R, Mariotti C, Uziel G, Smiderle C, Zeviani M. Mutations in TTC19 cause mitochondrial complex III deficiency and neurological impairment in humans and flies. Nat Genet. 2011; 43:259–263. [PubMed: 21278747]
31. Soto IC, Fontanesi F, Liu J, Barrientos A. Biogenesis and assembly of eukaryotic cytochrome c oxidase catalytic core. Biochim Biophys Acta. 2012; 1817:883–897. [PubMed: 21958598]
32. Weraarpachai W, Antonicka H, Sasarman F, Seeger J, Schrank B, Kolesar JE, Lochmuller H, Chevrette M, Kaufman BA, Horvath R, Shoubridge EA. Mutation in TACO1, encoding a translational activator of COX I, results in cytochrome c oxidase deficiency and late-onset Leigh syndrome. Nat Genet. 2009; 41:833–837. [PubMed: 19503089]
33. Weraarpachai W, Sasarman F, Nishimura T, Antonicka H, Aure K, Rotig A, Lombes A, Shoubridge EA. Mutations in C12orf62, a factor that couples COX I synthesis with cytochrome c oxidase assembly, cause fatal neonatal lactic acidosis. Am J Hum Genet. 2012; 90:142–151. [PubMed: 22243966]
34. Zara V, Conte L, Trumpower BL. Identification and characterization of cytochrome bc(1) subcomplexes in mitochondria from yeast with single and double deletions of genes encoding cytochrome bc(1) subunits. Febs J. 2007; 274:4526–4539. [PubMed: 17680808]
35. Ghezzi D, Goffrini P, Uziel G, Horvath R, Klopstock T, Lochmuller H, D'Adamo P, Gasparini P, Strom TM, Prokisch H, Invernizzi F, Ferrero I, Zeviani M. SDHAF1, encoding a LYR complex-II specific assembly factor, is mutated in SDH-defective infantile leukoencephalopathy. Nat Genet. 2009; 41:654–656. [PubMed: 19465911]
36. Moreno-Lastres D, Fontanesi F, Garcia-Consuegra I, Martin MA, Arenas J, Barrientos A, Ugalde C. Mitochondrial complex I plays an essential role in human respirasome assembly. Cell Metab. 2012; 15:324–335. [PubMed: 22342700]
37. Zara V, Conte L, Trumpower BL. Biogenesis of the yeast cytochrome bc1 complex. Biochim.Biophys.Acta. 2009; 1793:89–96. [PubMed: 18501197]

HIGHLIGHTS

- Human LYRM7 is identified as the yeast Mzm1 functional homolog
- LYRM7/MZM1L is a new human Complex III assembly factor
- MZM1L is a UQCRFS1 chaperone, binding and stabilizing it prior to its translocation
- UQCRFS1 correct insertion to mature Complex III depends on MZM1L stoichiometry

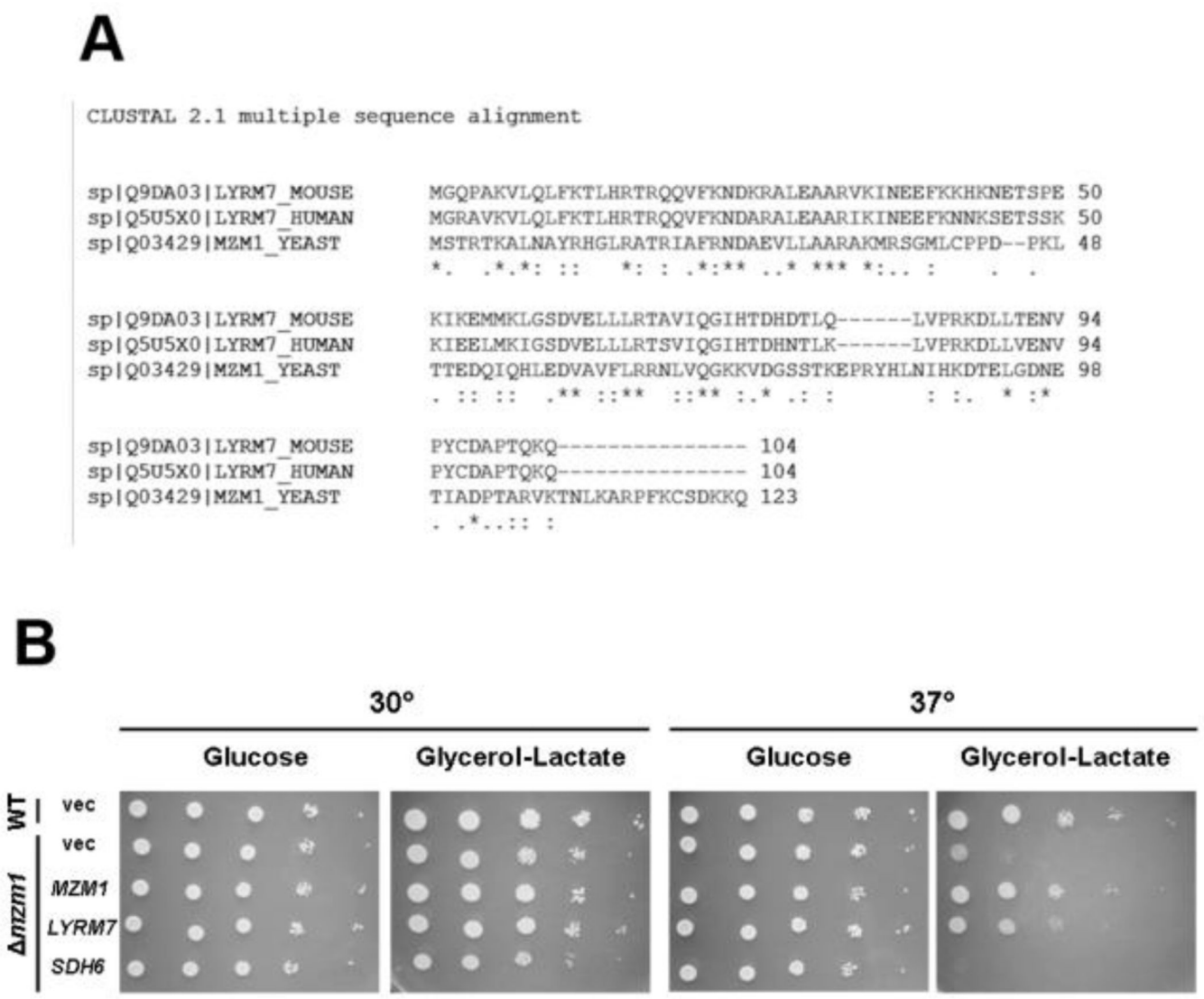

Figure 1.

LYRM7 as the yeast Mzm1p ortholog. A) Protein sequence alignment (ClustalW) of the yeast Mzm1 and human and mouse LYRM7, highlighting their high homology. The human protein displays 29% identity and 46% homology with the yeast protein. B) Growth assay of a yeast strain lacking endogenous Mzm1 and expressing exogenous human MZM1L. Wild-type (WT) and deletion mutant (Δ*mzm1*) yeast overexpressing plasmid-born yeast *MZM1*, human LYRM7 (MZM1L), yeast *SDH6* (an LYR protein with no known role in CIII assembly), or a vector control were spotted onto solid media plates at equivalent cell densities and serially diluted 10-fold four times. Plates were incubated at 30°C, a condition under which yeast show no growth phenotype in the absence of endogenous Mzm1 protein, and at 37°C, a stress condition under which growth in the absence of Mzm1 is severely retarded.

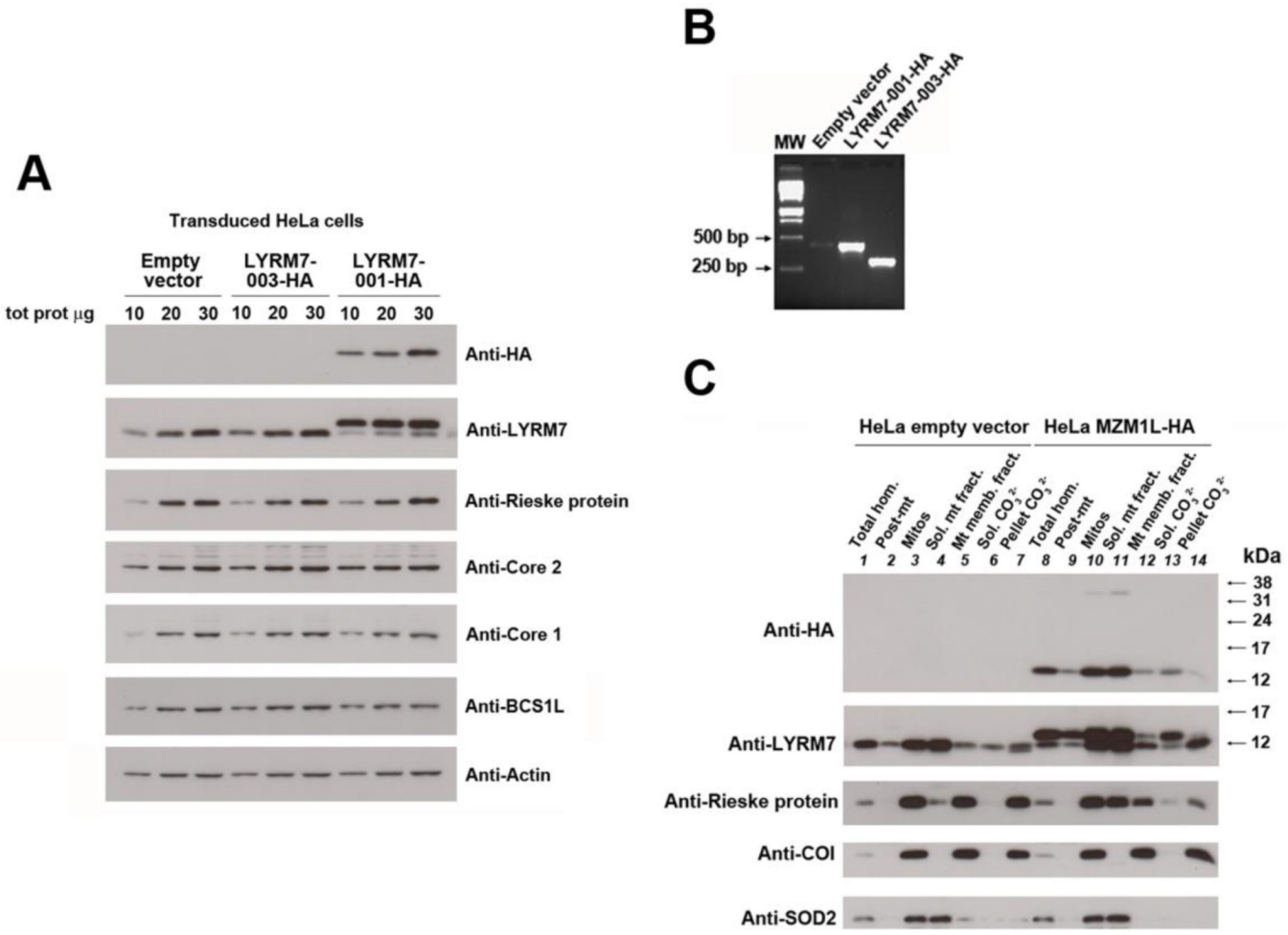

Figure 2.

Characterization of the tagged LYRM7 constructs: expression and localization of the protein product. A) SDS-PAGE and Western Blot of 3 different total protein amounts (10, 20 and 30 μg) extracted from HeLa cells transduced with the pWPXLd-ires-Puro^R empty vector and the LYRM7-003-HA/pWPXLd-ires-Puro^R and LYRM7-001-HA/pWPXLd-ires-Puro^R constructs. The blots were immunodetected with the indicated antibodies. B) PCR products amplified from cDNA, which was obtained from total RNA extracted from HeLa cells that were transduced with the pWPXLd-ires-Puro^R empty vector and the LYRM7-001-HA/pWPXLd-ires-Puro^R and LYRM7-003-HA/pWPXLd-ires-Puro^R constructs, using the hLYRM7-MluI-Fw primer and an oligonucleotide recognizing the HA sequence included at the end of each insert (5'-CAAGCGTAATCTGGAACATCG-3'). The amplification products showed the expected sizes for LYRM7-001-HA (416 bp) and for LYRM7-003-HA (300 bp). C) SDS-PAGE, Western Blot and immunodetection of proteins in different cellular fractions from HeLa cells transduced with the pWPXLd-ires-Puro^R empty vector and the LYRM7-001-HA/pWPXLd-ires-Puro^R (MZM1L-HA): Total cell homogenate (Total hom.), post-mitochondrial supernatant (Post-mt), isolated mitochondria (Mitos), soluble mitochondrial subfraction (Sol. mt fract.) and mitochondrial membrane fraction (Mt memb. fract.). The blots were immunodetected with the indicated specific antibodies. SOD2 and MT-CO1 were detected as markers for the mitochondrial matrix (soluble protein) and the mitochondrial membranes (inner membrane integral protein), respectively.

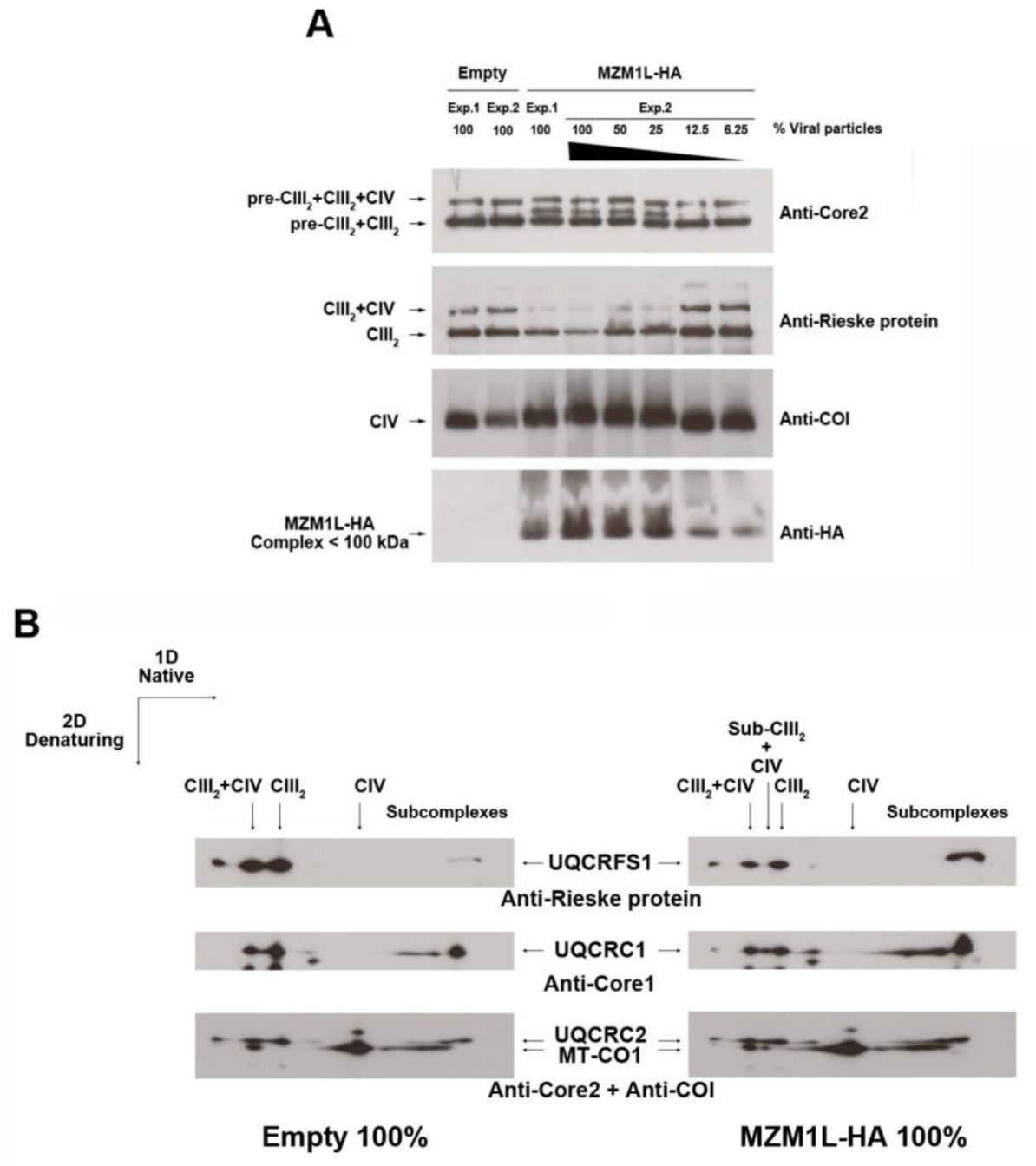

Figure 3.

Complex III assembly and activity in the transduced cells. A) First dimension (1D) BNGE and immunoblot analyses of samples prepared from HeLa cells transduced with the empty vector and with the MZM1L-HA construct. Samples are shown from two different experiments: Experiment 1, in which all the generated lentiviral particles were used to transduce the cells, and Experiment 2, where different proportions of the total virus titration (as indicated in the figure) were used to infect the cells, in order to modulate the MZM1L-HA expression levels. Antibodies against subunits UQCRC2 (Core 2) and UQCRFS1 (Rieske protein) were used to evaluate CIII assembly. Anti-HA was used to detect MZM1L-HA, and CIV was detected using anti-COI. B) Denaturing second dimension analysis after

the 1D BNGE of transduced HeLa cells with the empty control vector (left) and with the lentiviral vector expressing MZM1L-HA (right). Proteins in the blots were detected using the indicated specific antibodies.

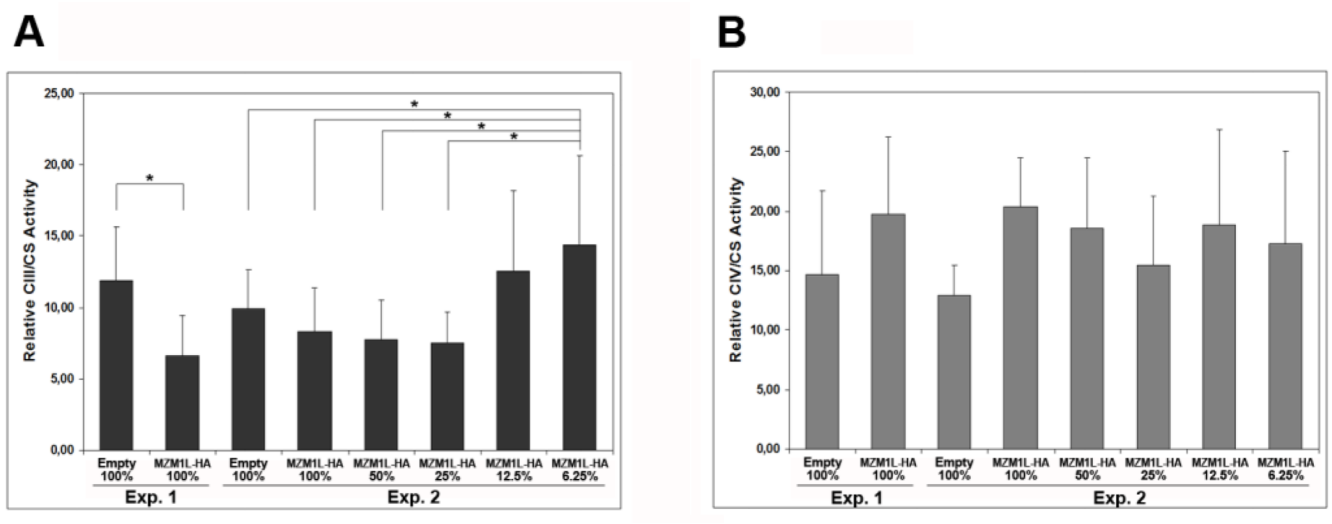

Figure 4.

Complex III (A) and Complex IV (B) enzymatic activities normalized to the Citrate Synthase activity (relative CIII/CS and relative CIV/CS activities) measured in the different transduced HeLa cell lines. Number 1 indicates cells from Experiment 1 and number 2 indicates cell lines from Experiment 2. The values plotted are the mean of four independent experiments (n = 4) ± SD. One way ANOVA analysis indicated statistically significant differences in the measured CIII/CS activities ($p = 0.018$) while no differences were found in CIV/CS activities ($p = 0.655$). Asterisks indicate statistically significant differences ($p < 0.05$) in the mean values between paired groups of data, according to the Post-Hoc LSD test.

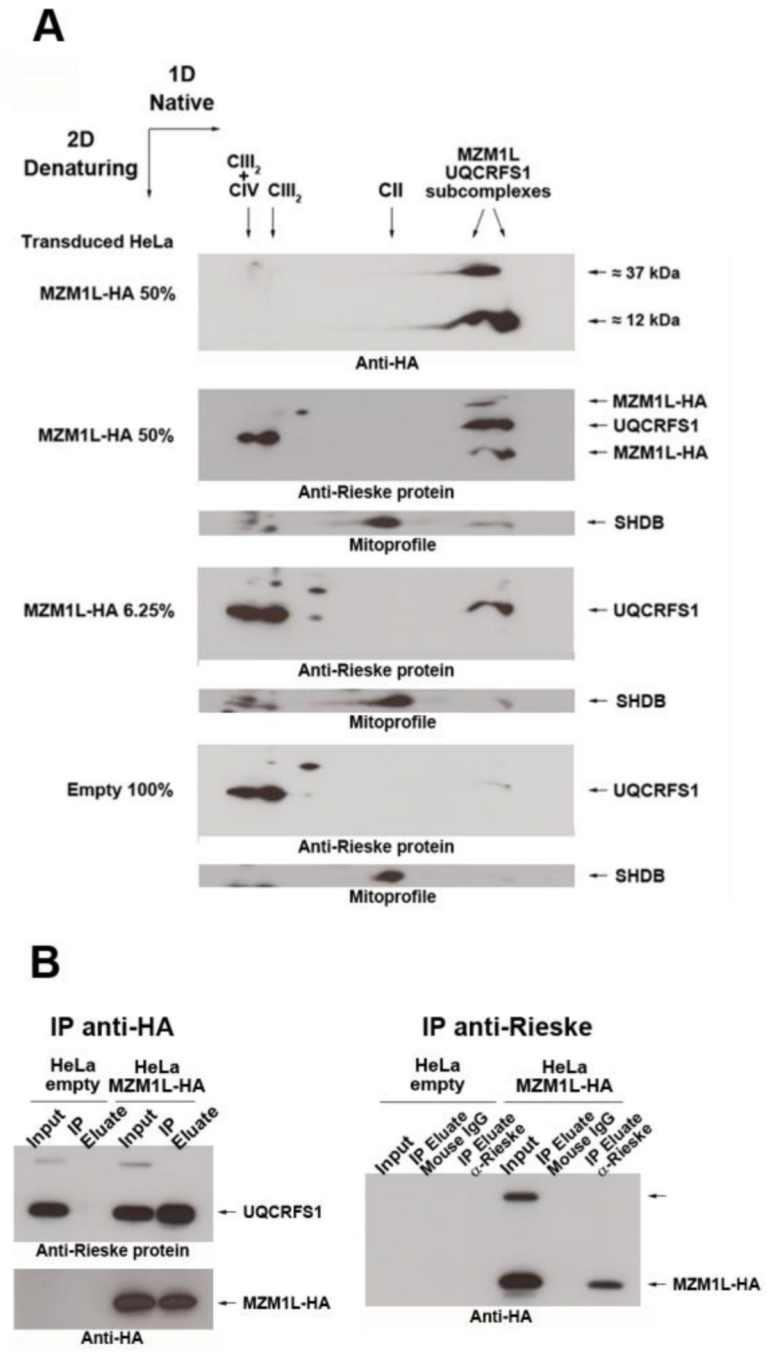

Figure 5.

Interaction between UQCRFS1 and MZM1L A) Denaturing second dimension analysis after the 1D BNGE of different transduced HeLa cell samples. Proteins in the blots were detected using the indicated specific antibodies. B) Co-immunoprecipitation analyses. Proteins in mitochondrial lysates from transduced HeLa cells were immunoprecipitated using the anti-HA antibody (left panel). The Western Blots after SDS-PAGE were immunodetected using anti-Rieske protein and polyclonal anti-HA antibodies (Invitrogen). The analysis indicated the presence of both proteins, UQCRFS1 and MZM1L-HA, in the co-immunoprecipitation eluate. On the other hand, proteins in mitochondrial lysates from transduced HeLa cells were immunoprecipitated using the anti-Rieske antibody, and as a control for unspecific binding,

generic mouse serum IgGs were used (right panel). The Western Blots after SDS-PAGE were immunodetected using anti-HA antibody. The analysis indicated the specific presence of MZM1L-HA in the same eluate when UQCRFS1 was immunoprecipated.

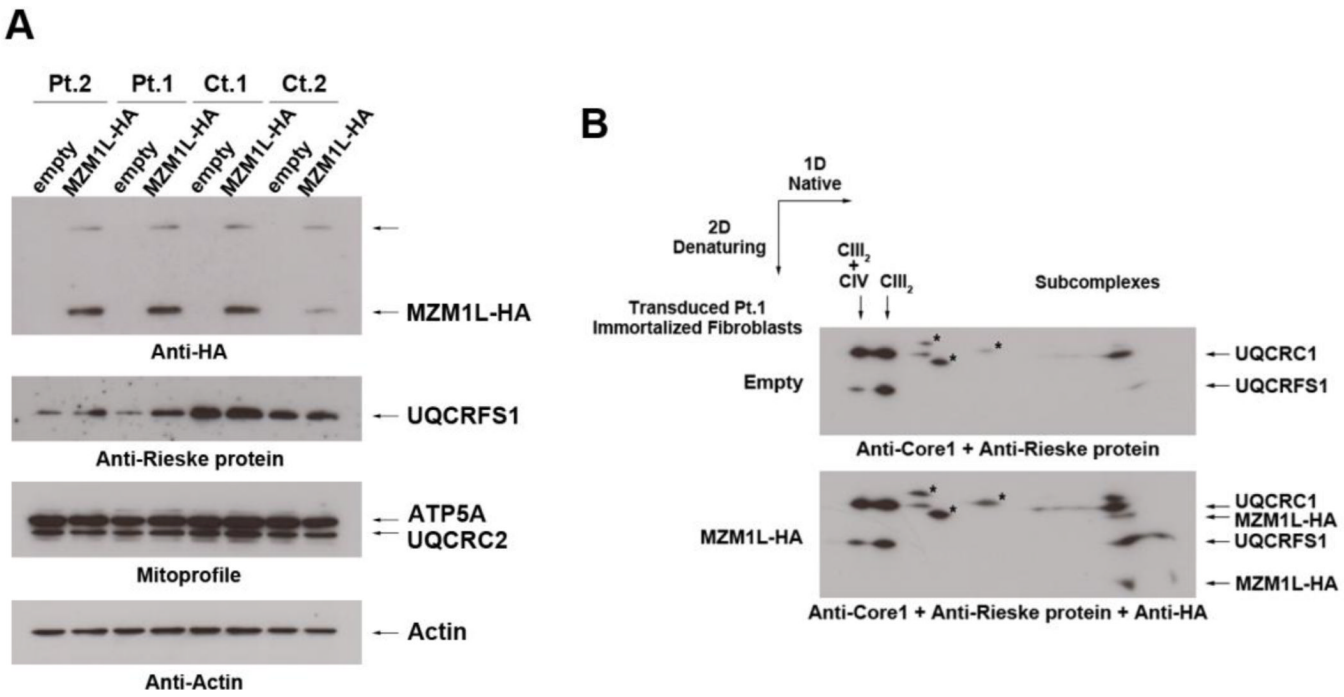

Figure 6.

Effects of MZM1L-HA overexpression in BCS1L mutated fibroblasts. A) SDS-PAGE, Western Blot and immunodetection analyses, with the indicated antibodies, of two patient (Pt) and two control (Ct) samples of immortalized fibroblasts transduced with either empty vector or MZM1L-HA. B) 2D BNGE, Western Blot and immunodetection analyses of the immortalized fibroblasts from Patient 1, which are compound heterozygotes of BCS1L mutations p.R73C and p.F368I [9], transduced either with the empty lentiviral vector or the MZM1L-HA construct. Asterisks indicate unspecific signals obtained with the anti-Rieske protein antibody.

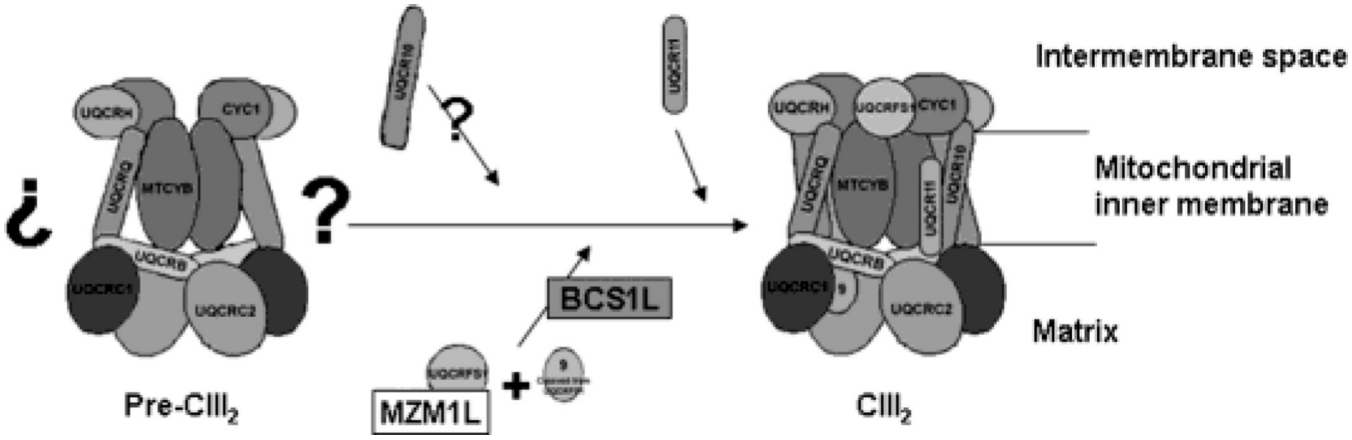

Figure 7.

Final steps of the putative mammalian CIII assembly pathway (inferred from the yeast model [37]), in which the newly identified factor LYRM7/MZM1L is now included. The question marks point out the current lack of knowledge on how the late core pre-$CIII_2$ is assembled in human mitochondria.